Magneto-electric optics in non-centrosymmetric ferromagnets

2008 J. Phys.: Condens. Matter 20 434211

(http://iopscience.iop.org/0953-8984/20/43/434211)

J. Phys.: Condens. Matter **20** (2008) 434211 (9pp) doi:10.1088/0953-8984/20/43/434211

Magneto-electric optics in non-centrosymmetric ferromagnets

T Arima

Institute of Multidisciplinary Research for Advanced Materials, Tohoku University, Sendai 980-8577, Japan
and
SPring-8 Center, RIKEN, Hyogo 679-5148, Japan

E-mail: arima@tagen.tohoku.ac.jp

Received 3 March 2008, in final form 23 May 2008
Published 9 October 2008
Online at stacks.iop.org/JPhysCM/20/434211

Abstract

Non-centrosymmetric ferromagnetic materials can show optical and x-ray responses unique to magneto-electrics. For example, the refractive index and absorption coefficient may be dependent on the directions of light (x-ray) propagation $\boldsymbol{k}$ and magnetization $\boldsymbol{M}$, and these dependences can be termed directional birefringence and directional dichroism, respectively. Such a kind of magneto-electric (ME) optics has recently been observed in $GaFeO_3$ and CuB_2O_4. The ME optics can be explained from the microscopic point of view by the interference of an electric dipole (E1) process with a magnetic dipole (M1) or electric quadrupole (E2) process at non-centrosymmetric magnetic sites. Even in magnetic crystals with global inversion symmetry, the E1–E2 interference can occur at magnetic sites with local inversion breaking, causing unique x-ray diffraction. Such ME-effect-related x-ray diffraction has been found in $GaFeO_3$ and Fe_3O_4. Artificial breaking of space inversion by means of currently used techniques such as lithography can be applied to the exploration of multiferroics, as a way of investigating ME optics. Relatively large ME optical signals at room temperature have been successfully observed in diffraction from such tailor-made multiferroics.

(Some figures in this article are in colour only in the electronic version)

1. Introduction

The symmetry of matter critically affects the interaction between the matter and light. For example, left- and right-handed circularly polarized light rays encounter a difference in the refractive and absorption coefficients in a medium that is non-superimposable on its mirror image; a so-called chiral medium. A similar optical response is also observed in a ferromagnetic solid, where the time reversal symmetry is broken. When both the space inversion and time reversal symmetries are simultaneously broken in a medium, novel optical effects are expected to be exhibited [1]. It is well known that such a magnetic material can exhibit the conventional linear magneto-electric (ME) effect. Electric polarization $\boldsymbol{P}$ is modulated by the application of a magnetic field $\boldsymbol{H}$, as

$$\Delta \boldsymbol{P} = \alpha \boldsymbol{H}. \tag{1}$$

Here, α is the linear ME tensor. Extending the relation to higher frequencies, ac magnetic fields ($\boldsymbol{H}^{\omega}$) with a frequency ω can generate an oscillating electric polarization ($\boldsymbol{P}^{\omega}$),

$$\boldsymbol{P}^{\omega}_{\mathrm{ME}} = \alpha(\omega)\boldsymbol{H}^{\omega}, \tag{2}$$

where $\alpha(\omega)$ is the ω-dependent complex ME tensor. As the frequency ω becomes as high as that of light or x-rays, equation (2) may contribute to the optical/x-ray response, which is referred to as optical ME effects or ME optics[1]. This is in very sharp contrast to the usual optical response, where the oscillating magnetic field of light $\boldsymbol{H}^{\omega}$ has almost no impact on the optical response.

One of the characteristics of ME optics is that the refractive index and absorption coefficient are expected to change in sign with the reversal of the propagation vector $\boldsymbol{k}$ of the electromagnetic wave. The optical response of a material

[1] The terminology for the unique optical response arising from the linear magneto-electric effect is somewhat confusing. In this paper, I use magneto-electric optics in the same manner as magneto-optics, electro-optics, piezo-optics and so on.

can be represented by the polarizability, defined as the ratio of $\boldsymbol{P}^{\omega}$ to $\boldsymbol{E}^{\omega}$. The geometric relation between $\boldsymbol{E}^{\omega}$ and $\boldsymbol{H}^{\omega}$ is governed by the propagation direction, as shown by Faraday's law,

$$\boldsymbol{H}^{\omega} = \frac{1}{\mu(\omega)\mu_0\omega}\boldsymbol{k} \times \boldsymbol{E}^{\omega}. \tag{3}$$

Thus, equation (2) becomes

$$\boldsymbol{P}^{\omega}_{\mathrm{ME}} = \frac{\alpha(\omega)}{\mu(\omega)\mu_0\omega}\boldsymbol{k} \times \boldsymbol{E}^{\omega}. \tag{4}$$

Equation (4) clearly indicates that the polarizability in this class of magnetic material contains a $\boldsymbol{k}$-odd component. As a consequence, the optical/x-ray response can be modified by the reversal of $\boldsymbol{k}$. Another property of ME optics is the odd nature of time reversal (strictly speaking, for the lossless case). The optical effect shown by equation (4) changes in sign with the reversal of all the spin and orbital momenta, as is the case for the linear ME effect. From this perspective, ME optics is a non-reciprocal effect.

Experimental evidence of spontaneous ME optics was first reported for a non-centrosymmetric antiferromagnet Cr_2O_3 by Pisarev *et al* [2, 3]. Chromium sesquioxide is a prototypical magneto-electric compound, in which the existence of the linear ME effect was first proved in the 1950s [4]. The magnetic point group of the antiferromagnetic state is described as $\bar{3}'m'$, indicating non-zero diagonal components $\alpha_{xx} = \alpha_{yy}$ and α_{zz} of the linear ME tensor α. Pisarev *et al* discovered a difference in the rotation of light between the two types of antiferromagnetic domains in Cr_2O_3, interchanged with each other by a time reversal operation [2]. Such a non-reciprocal optical effect was exactly what had been predicted and called 'non-reciprocal or gyrotropic birefringence' by Brown *et al* [1]. They also found circular dichroism (difference in absorption between two circularly polarized light rays) in the reflection of light from Cr_2O_3. The observed circular dichroism was opposite in sign for the two types of antiferromagnetic domains [3]. The discovered gyrotropic birefringence and circular dichroism are ascribed to the diagonal components of the linear ME tensor.

Gyrotropic birefringence is not the only form of ME optics. When an electromagnetic wave propagates in the $\pm z$ direction, four components of the linear ME tensor, α_{xx}, α_{xy}, α_{yx}, and α_{yy}, can give rise to ME optics. While gyrotropic birefringence and circular dichroism are generated by the average of α_{xx} and α_{yy}, as in the case of Cr_2O_3, differences in refractive index (birefringence) and in absorption (dichroism) between two kinds of linearly polarized light rays are expected to arise from a difference between α_{xx} and α_{yy}. A difference between two off-diagonal components α_{xy} and α_{yx} causes differences in refractive index and absorption coefficient with respective to the reversal of $\boldsymbol{k}$ regardless of the polarization of light, which can be termed directional birefringence/dichroism. The average of the two off-diagonal components α_{xy} and α_{yx} results in birefringence and dichroism for light linearly polarized along the x and y axes.

Non-centrosymmetric ferromagnetic materials with various magnetic point groups possess the above-mentioned different types of linear ME tensors [5]. In ferroelectric ferromagnets, or multiferroics in the original definition, the geometrical relation between magnetization $\boldsymbol{M}$ and electric polarization $\boldsymbol{P}$ controls which components of α can appear. In a ferroelectric, or more generally, a polar material with $\boldsymbol{M}$ parallel to $\boldsymbol{P}$, the diagonal components of α should be non-zero. Gyrotropic birefringence and circular dichroism are thus expected in such a material. In contrast, when $\boldsymbol{M}$ is perpendicular to $\boldsymbol{P}$, at least two off-diagonal components are expected to be non-zero. Directional birefringence/dichroism and linear birefringence/dichroism are expected to be exhibited for light propagating in the $\boldsymbol{P} \times \boldsymbol{M}$ direction. Here, it is worth noting that the vector product of $\boldsymbol{P}$ and $\boldsymbol{M}$ is closely related to a toroidal moment [6], which is discussed in detail by Fiebig *et al* [7]. The spin part of the toroidal moment $\boldsymbol{T}$ is described as $\boldsymbol{T} \propto \sum_n \boldsymbol{r_n} \times \boldsymbol{S_n}$, where $\boldsymbol{S_n}$ is the spin of the n magnetic ion at the position $\boldsymbol{r_n}$. On the other hand, in a point charge approximation, $\boldsymbol{P} \times \boldsymbol{M} \propto \sum_{n,n'} \rho_{n'} \boldsymbol{r}_{n'} \times \boldsymbol{S_n}$, where $\rho_{n'}$ is the charge of the ion n' at $\boldsymbol{r}_{n'}$. In fairly simple cases, we can therefore consider $\boldsymbol{T} \propto \boldsymbol{P} \times \boldsymbol{M}$, and then, dichroism is expected for light propagating parallel and anti-parallel to $\boldsymbol{T}$.

Closely associated with ME optics is an interesting magneto-optic effect termed the magneto-chiral effect. This effect appears as a change in the optical indices in a chiral medium subject to an external magnetic field $\boldsymbol{H}$ parallel to $\boldsymbol{k}$. It is of note that the magneto-chiral susceptibility has opposite signs for the two enantiomers (mirror images) of a chiral medium [8]. This is, however, independent of the state of polarization of the light. The magneto-chiral birefringence and dichroism can be regarded as being a kind of ME optic effect in magnetized chiral media, except that the magnetization is not spontaneous but induced by an external magnetic field. In fact, in chiral ferromagnets, as some off-diagonal components can become non-zero, non-reciprocal directional birefringence and dichroism can be observed for the configuration of $\boldsymbol{k} \parallel \boldsymbol{M}$.

2. Non-reciprocal directional dichroism

2.1. Non-reciprocal directional dichroism in $GaFeO_3$

Gallium iron oxide $GaFeO_3$, which was first synthesized by Remeika [9], is a well-known piezoelectric ferrimagnetic material. $GaFeO_3$ has an orthorhombic unit cell with spontaneous polarization along the b axis, as schematically shown in figure 1. The ferrite undergoes a ferrimagnetic transition with the magnetic easy axis of c. In the magnetic phase, the magnetic space group is $Pc'2'_1n$, where the group theory predicts the linear ME response with the tensor components of α_{bc} and α_{cb}. Observation of the ME effect was first reported by Rado in 1964 [10].

Non-zero α_{bc} and α_{cb} in $GaFeO_3$ are expected to cause directional birefringence and dichroism for an electromagnetic wave propagating along the a axis. Kubota *et al* have observed x-ray non-reciprocal directional dichroism (XNDD) in the vicinity of the Fe K-absorption edge by applying the magnetic field modulation technique [11]. The lower panel of figure 2(a) shows XNDD spectra for $GaFeO_3$ in the ferrimagnetic phase for two polarizations of x-rays, $\boldsymbol{E}^{\omega} \parallel b$ and $\boldsymbol{E}^{\omega} \parallel c$, corresponding to the imaginary parts of the ME coefficients

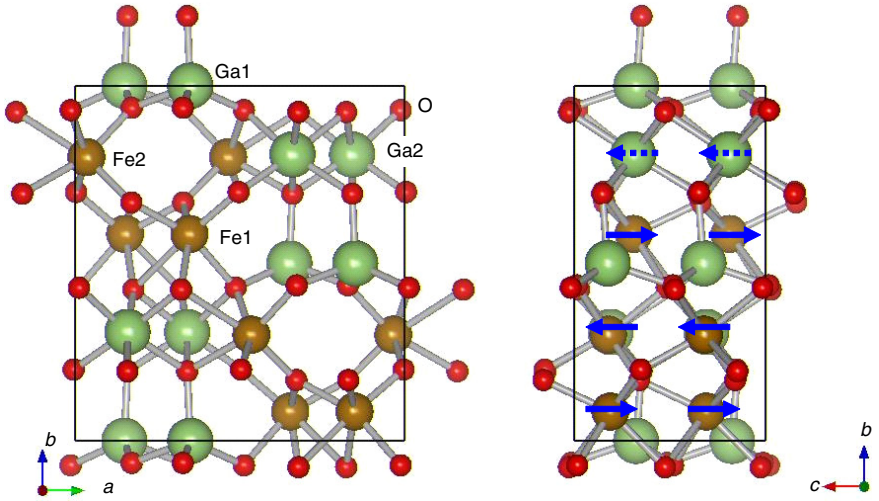

Figure 1. Crystal and magnetic structure of $GaFeO_3$ crystal with a space group of $Pc2_1n$. Projection views along (left) c and (right) a axes. An electric polarization appears along the 2_1 screw b axis, which causes breaking of inversion symmetry. The magnetic structure is ferrimagnetic with a magnetic point group of $m'2'm$ below T_C. The c axis is a magnetic easy axis and the saturated moment is about 0.6 μ_B/Fe.

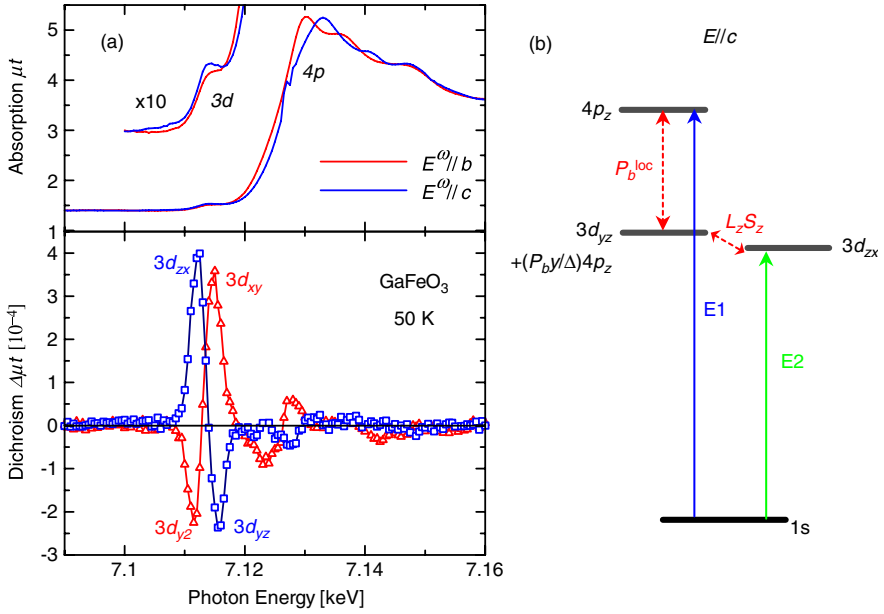

Figure 2. (a) Spectra of x-ray (upper) absorption and (lower) non-reciprocal directional dichroism (XNDD) in a $GaFeO_3$ crystal at 50 K for x-ray polarizations parallel to the b and c axes. XNDD is defined as the difference in absorption coefficient between when a magnetic field is applied parallel ($H+$) and anti-parallel ($H-$) to the c axis. (b) Energy-level diagrams for explaining the XNDD spectra for $GaFeO_3$ for x-ray polarization parallel to the c axis. Excerpts from [11]. Reprinted with permission from [11]. Copyright 2004 by the American Physical Society.

α_{bc} and α_{cb}, respectively. A few resonant peaks of the order of 0.01% are noticeable. The resonance is larger for the small absorption shoulder below 7.12 keV corresponding to the 1s–3d excitation, than for the absorption edge at 7.12–7.13 keV assigned to the 1s–4p excitation. The overall features of the spectra are successfully explained by a simple FeO_6 octahedron cluster model. The 3d states are roughly split into three-fold t_{2g}-like states and two-fold e_g-like states by the crystal field. 1s–3d excitation usually originates from an electric quadrupole (E2) process, because both the 1s and 3d orbitals have an even parity. At the non-centrosymmetric sites, however, an electric dipole (E1) process can also contribute to the 1s–3d excitation. One can suppose that the potential gradient for the spontaneous polarization, which is parallel to the b axis, should be relevant to XNDD in a polar ferrimagnet $GaFeO_3$. The final 3d state of the E1 transition from the 1s state is not identical to that of the E2 transition for the electromagnetic wave propagating along the a axis. For example, the former is $3d_{yz}$, while the latter is $3d_{zx}$, when the wave is polarized along the c axis, as indicated in figure 2(b).[2]

[2] Here, I take the Cartesian x, y, and z coordination parallel to a, b, and c, respectively.

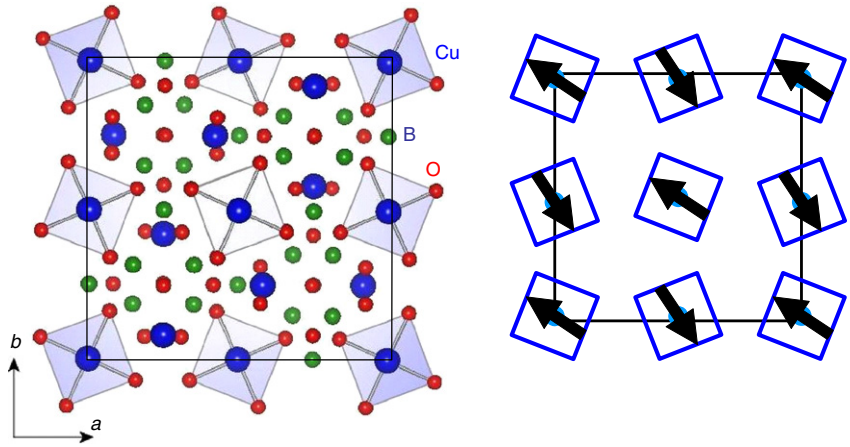

Figure 3. Crystal and magnetic structures of CuB_2O_4 projected along the c axis. (Left) Red and green spheres represent oxygen and boron, respectively. Cu atoms (blue) occupy two non-equivalent positions. Cu atoms on the A-sites coordinated by four oxygen atoms are shown by light blue squares. (Right) Alignments of magnetic moments of Cu^{2+} ions on the A-sites in a magnetic field along the [110] axis.

With the spin moment aligned along the c axis, the spin–orbit interaction gives rise to a matrix element between the two final states. As a consequence, the E1 and E2 processes interfere with each other in a constructive or destructive way, depending on the spin orientation. A part of the spectral weight is hence transferred between the 1s–3d_{yz} and 1s–3d_{zx} transitions. The positive signal at 7.16 keV and the negative one at 7.18 keV can be attributed to the spectral-weight transfer. Needless to say, the XNDD signal corresponds to the sum of this interference over all the Fe sites. There are two crystallographically independent Fe^{3+} sites, Fe1 and Fe2, in $GaFeO_3$. Both the sites are shifted from the centers of oxygen octahedra. The b components of the displacements are $+0.26$ Å and -0.11 Å for Fe1 and Fe2 sites, respectively [12]. Since the spin moments on Fe1 and Fe2 along the c axis are antiferromagnetically aligned below T_N, the vector product of the shift and spin moment on Fe1, which is also termed a toroidal moment [6], is in the same direction along the a axis as that on Fe2. The clear XNDD signal for $GaFeO_3$ could be ascribed to the ferro-toroidic nature of $GaFeO_3$, as Popov *et al* have pointed out as a possible origin of the static ME effect in $GaFeO_3$ [13]. In other words, XNDD can be used to element-selectively detect ferro-toroidicity, which is becoming a hot topic in the field of multiferroics [14]. More quantitative calculations of XNDD in $GaFeO_3$ have been performed by Matteo *et al* [15, 16]. They estimated the contribution of other moments such as electric/magnetic dipoles, quadrupoles, and octupoles to x-ray absorption and diffraction.

Similar interference in magneto-electrics is also expected between the magnetic dipole (M1) and E1 processes for the intra-atomic 3d–3d excitation, which would resonate with near-infrared or visible light. In fact, Jung *et al* have reported non-reciprocal directional dichroism (NDD) of near-infrared and visible light in $GaFeO_3$ [17]. The NDD spectra for linearly polarized light are rather broad and have not been well analyzed yet, partly because of the very low local symmetry at the Fe^{3+} sites. Each Fe site has no symmetry operations, which means the E1 and M1 processes are allowed for transitions to any excited states. The magnitude of the NDD signal is of the order of 0.1% and follows the magnetization well as a function of temperature.

2.2. *Non-reciprocal directional dichroism in CuB_2O_4*

Copper metaborate CuB_2O_4 is a non-centrosymmetric tetragonal system with a space group $I\bar{4}2d$. The cuprate has a transparent blue color due to the intra-atomic d–d transitions at $3d^9$ Cu^{2+} ions, which occupy two crystallographic sites: square planar Cu(A) and heavily distorted octahedral Cu(B) sites (see figure 3). The electron transfer between Cu ions is thought to be small, because all the clusters (CuO_4 squares and CuO_6 octahedra) are separate from one another without sharing any oxygen atoms. As a result, copper metaborate is a magnetic insulator, where each Cu^{2+} ion behaves as a local $S = 1/2$ spin moment. With decreasing temperature, the compound undergoes successive magnetic transitions [18]. At around 20 K, a steep rise in magnetization is observed. A neutron study has proposed that magnetic moments on Cu(A) sites are antiferromagnetically aligned and slightly canted through the so-called Dzyaloshinskii–Moriya (DM) interaction with the DM vector along the c axis, as depicted in the right panel of figure 3. The weak ferromagnetic moment disappears below 10 K. Although the magnetic structure in the low-temperature phase has not yet been clarified, some experimental studies support incommensurate helical magnetism with the propagation vector parallel to the c axis [18, 19].

In the canted antiferromagnetic phase with spontaneous magnetization along the [110] axis, the magnetic space group is $I2'dd'$, indicative of the presence of the off-diagonal ME susceptibilities. Saito *et al* have recently studied NDD for linearly polarized light propagating along the [1$\bar{1}$0] axis [20]. The optical absorption at 1.405 eV resonating with a intra-atomic $d_{x^2-y^2}$–d_{xy} transition of a Cu^{2+} hole shows NDD with the light polarizing normal to the c axis, as can be seen in figure 4. The magnitude of the absorption changes by a factor of three with the reversal of magnetization direction. This extraordinarily large effect originates from the interference between an M1 process and an originally forbidden E1 process

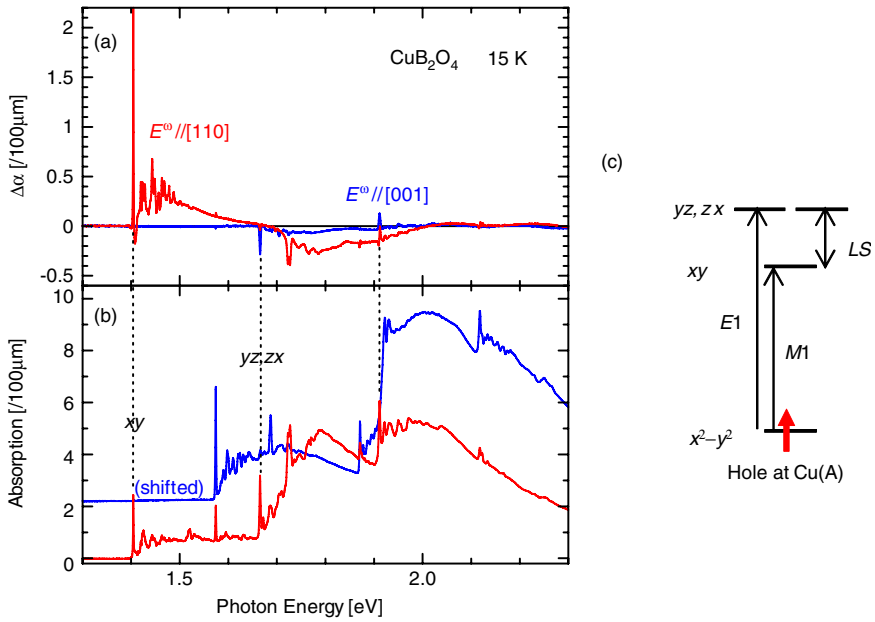

Figure 4. Spectra of (a) non-reciprocal directional dichroism (NDD) and (b) absorption in CuB_2O_4 at 15 K for light polarizations normal and parallel to the *c* axis. Excerpt from [20], reprinted with permission. Copyright 2008, Institute of Pure and Applied Physics. (c) Energy-level diagrams for explaining NDD in CuB_2O_4 for light polarization normal to the *c* axis.

assisted by the weakly broken space inversion via the spin–orbit interaction. The NDD signal continues for the higher-lying phonon-side bands from 1.405 to 1.67 eV, and changes sign for another intra-atomic transition band from $d_{x^2-y^2}$ to the doubly degenerate d_{yz} and d_{zx} orbitals. The sign change can be attributed to the spectral-weight transfer between the M1-allowed $d_{x^2-y^2}$-to-d_{xy} transition and the weakly E1-allowed $d_{x^2-y^2}$-to-d_{yz}, -d_{zx} transitions. The discovery of large NDD will open up new possibilities of novel optical devices.

3. Magneto-electric emission of light

If a medium exhibiting a linear ME effect shows luminescence, the intensity of emission could depend on the direction of emitted light through a possible ME optical effect. The existence of an ME optical effect exhibiting luminescence would have an impact on the technology of optics. However, such light-emitting magneto-electrics have yet to be discovered, to the best of the author's knowledge. Nevertheless, a similar effect has been achieved by the application of a relatively strong field to non-centrosymmetric and paramagnetic light-emitting media. More than a decade ago Rikken and Raupach first reported magneto-chiral dichroism in emission [21]. Luminescence from Eu^{3+} ions in a chiral $Eu((\pm)tfc)_3$ complex dissolved in deuterated dimethyl sulfoxide changes by approximately 0.1% with the application of a magnetic field of 0.9 T. The magnitude of the magneto-chiral signal is proportional to the strength of magnetic field and differs in sign between the two enantiomers. Shimada *et al* have recently reported a magnetic-field-induced ME effect on emission from rare earth doped ferroelectrics [22, 23]. The field-induced ME effect resulting in the Er^{3+} $^4I_{15/2}$-to-$^4I_{13/2}$ emission from Er^{3+}-doped $La_2Ti_2O_7$ is displayed in figure 5. The sign of the magnetic field modulation is found to change due to the reversal of the ferroelectric polarization. Many peaks should correspond to the crystal field splitting of the multiplets in the excited and ground states, though it is difficult to assign them explicitly.

4. Magneto-electric diffraction

4.1. Magneto-electric x-ray diffraction

When magnetic moments are periodically aligned in a medium, magnetic diffraction of neutrons and x-rays can be seen. Arrangement of toroidal moments could similarly be investigated by using a diffraction technique. As toroidal moments should induce interference between E1 and E2 processes, resonant x-ray diffraction would be a good probe for investigating toroidal ordering.

A first trial for the x-ray detection of toroidal moments has been performed for $GaFeO_3$ [24]. Considering the crystal structure of $GaFeO_3$ as a layered structure, Fe1 and Fe2 layers are alternately stacked along the *b* axis. On the one hand, the arrangement of spin moments has the propagation vector of (020) with a parasitic component at (040), corresponding to the ferromagnetic moment. As for the toroidal moments, on the other hand, the main Fourier component has a wavevector of (040) because of its ferro-toroidic nature, as previously described. The (020) component is not very small because the absolute values of the atomic displacements of Fe1 and Fe2 sites differ by a factor of 2.5. Modulation of the intensities of diffraction at (020) and (040) with an ac magnetic field applied along the magnetic easy axis (*c*) has been investigated for linearly polarized x-rays with $\boldsymbol{E}^\omega$ parallel to the ac magnetic field. In this configuration, both purely magnetic and magneto-electric diffractions are allowed. The former mainly stems from an M1 process, which must be nearly independent of the photon energy, while the latter is expected to show a

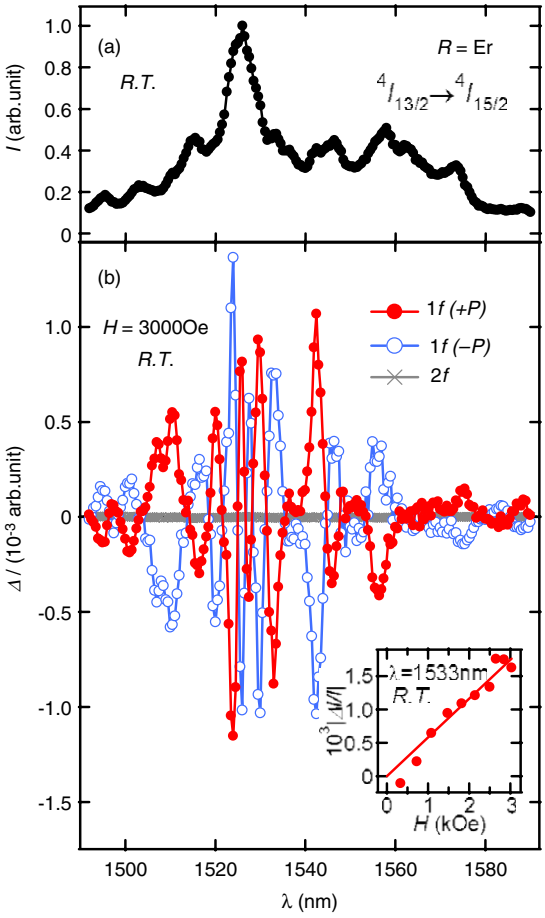

Figure 5. (a) Emission spectrum of Er-doped $La_2Ti_2O_7$ at room temperature. Intensity of emission I is normalized using the maximum value at around the wavelength λ of 1526 nm. (b) Optical ME spectra with ac magnetic field ($f = 5$ Hz) of $H = 3000$ Oe for the $P \perp H$ and $k \parallel P \times H$ configuration. The ΔI spectra defined as the ac modulated amplitude of I are normalized using the same scale of emission (I) spectrum. The 1f component of ΔI for the $+P$ configuration and the 1f component of ΔI for the $-P$ configuration are represented by filled and open circles, respectively. The 2f component of ΔI is represented by cross symbols. The inset shows the H dependence of the signal $\Delta I/I$ at $\lambda = 1533$ nm. The solid line is a linear fit. Excerpt from [23]. Reprinted with permission from [23]. Copyright 2007 by the American Physical Society.

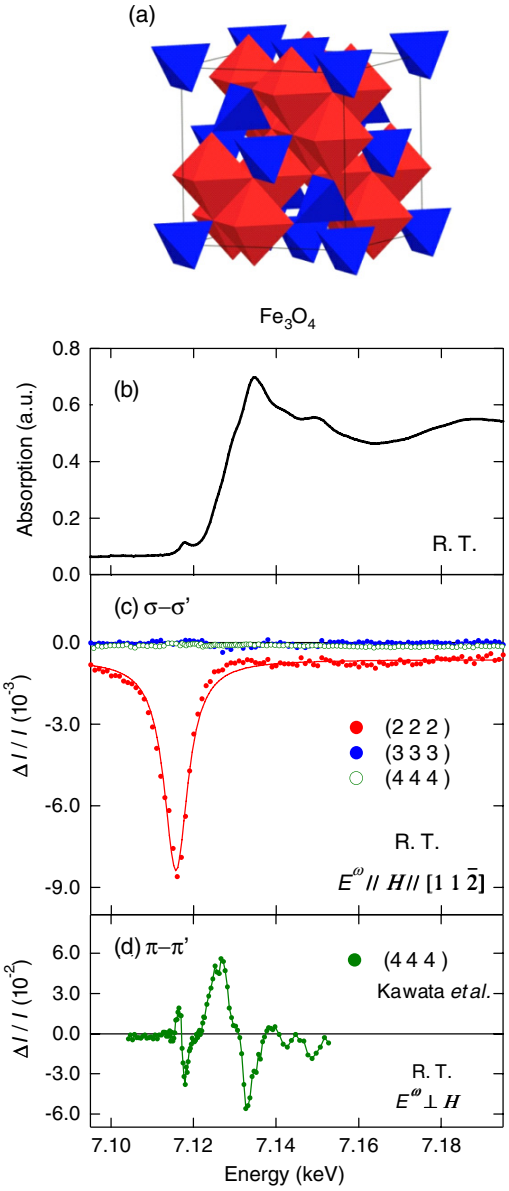

Figure 6. Various x-ray spectra for Fe_3O_4 in the vicinity of the Fe K-absorption edge at room temperature. (a) Absorption spectrum of pulverized crystal. (b) Magnetic scattering spectra (including those from magneto-electric processes) $\Delta I/I$ for (222) (red), (333) (blue), and (444) (green) reflections for $\boldsymbol{E}^{\omega} \parallel \boldsymbol{H} \parallel [11\bar{2}]$ in the σ–σ' scattering process; (c) magnetic scattering spectrum for the (444) Bragg reflection for $E \perp H$ in the π–π' scattering process, quoted from [26]. Solid lines in (b) and (c) are merely guides for the eyes. Excerpt from [25]. Reprinted with permission from [25]. Copyright 2005 by the American Physical Society.

resonant behavior with the 1s–3d transition. As predicted, the non-resonant purely magnetic diffraction at (020) and strongly resonant ME diffractions at (020) and (040) are clearly observed.

ME x-ray diffraction has a unique advantage over XNDD: it can also, in principle, be used to detect antiferroic ordering of local ME sources such as toroidal moments. This is quite similar to the relation between x-ray magnetic circular dichroism, which is used to detect ferromagnetic moments, and x-ray magnetic diffraction, which is useful in investigating antiferromagnetism. Resonant ME x-ray diffraction can be used as a unique probe into magnetism, because it has both an element-selective nature and a site-selective nature. Magnetic moments at centrosymmetric sites do not show any x-ray ME effect.

Such an approach has been reported by Matsubara *et al*, who have intensively studied resonant magnetic x-ray scattering in a crystal of spinel-type magnetite [25]. The spinel structure contains tetrahedral A-sites and octahedral B-sites as depicted in figure 6(a). When the tetrahedral A-sites are occupied by magnetic ions, local space inversion and time reversal symmetries are simultaneously broken. In the cubic spinel, the tetrahedral A-sites do not possess an electric dipole but an octupole. The electric octupole moments are arranged in the antiferroic manner. On the other hand, it is well known that the Fe^{3+} spin moments on the tetrahedral A-sites are ferromagnetically ordered at room temperature. Some moment

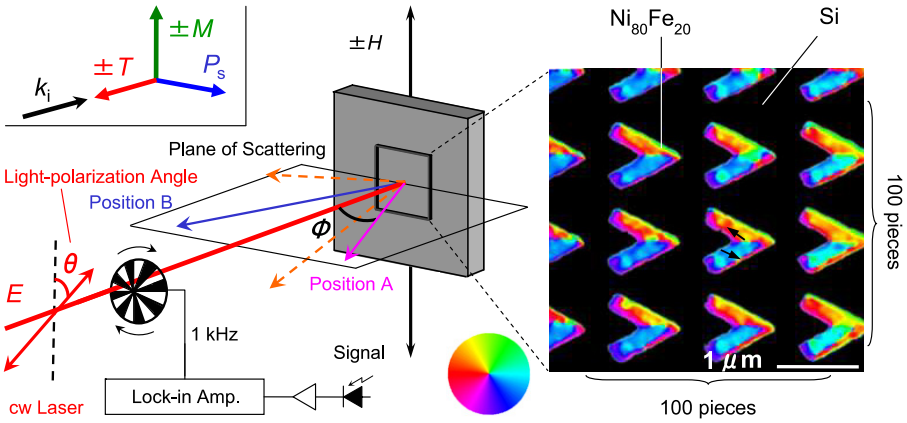

Figure 7. Experimental setup for the observation of the optical ME effect by diffraction measurements. Four Bragg diffractions of the order $n = \pm 1$ appear at the diffraction angle ϕ of $\sim 40°$ when the light from the laser diode (wavelength λ of 785 nm) is irradiated on the sub-micron-scale patterned magnet sample (see right panel) at normal incidence. Diffracted light is phase-sensitively detected by a silicon photodiode at positions A and B. A static magnetic field $\boldsymbol{H}$ is applied perpendicular to the plane of scattering. A spin-polarized scanning electron microscopy (SEM) image obtained at room temperature of the non-centrosymmetric chevron-shaped patterns, which was recorded after the removal of $\boldsymbol{H}$ of 500 Oe, is shown in the right panel. The relationship between the color and the direction of the in-plane remnant magnetization is represented by the color wheel; the direction of the remnant magnetization is also indicated by black arrows in one of the patterns in the spin-polarized SEM image. The black background area corresponds to the silicon substrate. Upper left inset shows the configuration of toroidal $\boldsymbol{T}$. The propagation vector $\boldsymbol{k}_i$ of incident light is set parallel or anti-parallel to $\boldsymbol{T}$. Excerpt from [27]. Reprinted with permission from [27]. Copyright 2005 by the American Physical Society.

defined as the product of electric octupole and magnetic dipole moments therefore undergoes antiferroic ordering. This complex moment can also induce interference between E1 and E2 processes. Spectra of absorption and magneto-electric scattering are shown in figure 6. A fairly large ME signal is successfully observed at (222) in Fe_3O_4 at room temperature (see figure 6(b)), which is in accord with the antiferroic ordering of the complex moments. The (222) spectrum is clearly different from the spectrum of magnetic diffraction at (444) in figure 6(c) taken from [26], providing evidence that the ME diffraction arises from E1–E2 interference, which does not resonate with the 1s–4p transition. In contrast, the magnetic x-ray diffraction in the π–π' polarization channel mainly originates from E1–E1 interference. The larger structure above 7.12 keV in the (444) magnetic diffraction spectrum should be attributed to this interference.

4.2. Magneto-electric diffraction of light in patterned magnets

As discussed above, it has been established that non-centrosymmetric crystals can exhibit observable ME optical phenomena. Other approaches to the realization of ME optics are also significant, because to date few non-centrosymmetric ferromagnetic materials have been reported. One promising approach is the fabrication of a (sub-)micrometer-scale artificial magnetic superstructure with a non-centrosymmetric shape, where both the space inversion and time reversal are expected to be simultaneously broken. The superstructure would induce the ME diffraction of visible light, which has a wavelength comparable to its period. The ME diffraction can be made to appear at room temperature by utilizing a ferromagnet with a high Curie temperature as a component. Moreover, currently used lithography techniques enable one to control the size, shape, and period of such a superstructure.

The first successful approach was reported by Kida *et al* [27]. They fabricated a superstructure consisting of a two-dimensional periodic array of 100 × 100 chevron-shaped sub-micron-scale patterns made of ferromagnetic Permalloy on a Si substrate (see figure 7). This tailor-made superstructure lacks space-inversion symmetry due to the asymmetric shape of the chevrons. This also breaks the time reversal symmetry due to the ferromagnetic nature of Permalloy. The observed optical ME diffraction signal at room temperature is about 10^{-3} in a magnetic field of 500 Oe; this being comparable with the magnitude of the conventional magneto-optical Kerr effect.

Another advantage of the artificial patterns would be possible enhancement of the signal. After Sawada and Nagaosa proposed that a photonic crystal made of multiferroics would enhance ME susceptibility [28], Kida *et al* studied such ME diffraction of light from a periodic grating on a multiferroic $GaFeO_3$ [29]. They fabricated a grating with a pitch of 4 μm and a height of 150 nm on a (010) surface of a single crystal of $GaFeO_3$, as shown in figure 8. The intensities of diffracted beams are modulated by the application of a magnetic field, as expected. The magnitude of the ME modulation of the diffraction intensity exceeds 1%. Here, it is worth noting that the incident laser with $\boldsymbol{k} \parallel b$ is not subject to the ME susceptibility. The observed modulation should be ascribed to the ME response of the diffracted beam, because the propagation vector of the diffracted beam $\boldsymbol{k}_{\rm out}$ is not normal to the toroidal $\boldsymbol{T}$ of $GaFeO_3$ (see figure 8). Care should be taken to distinguish this situation from the case of the above-mentioned chevron array, where the optical indices of the incident beam should be affected by the simultaneous breaking of inversion and time reversal symmetries of matter.

A similar ME grating can also be fabricated from an ABCABC$\cdots$-type asymmetric magnetic superlattice (SL). Scientists are now aware that an effective electric polarity

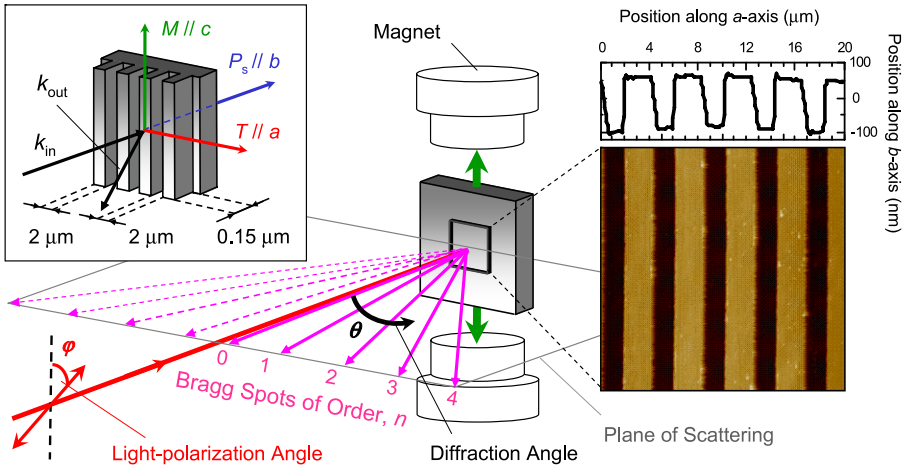

Figure 8. Schematic illustration of a fabricated multiferroic grating and the magneto-optical setup in the transverse geometry for diffraction experiments, where the magnetic field was applied perpendicular to the plane of scattering. A detector placed on a goniometer was rotated within the plane of scattering so as to satisfy Bragg's diffraction law. The relationships among the propagation vector $\boldsymbol{k}_{\rm in}$ of incident light, $\boldsymbol{k}_{\rm out}$ of diffracted light, the spontaneous polarization $\boldsymbol{P}_s$, the magnetization $\boldsymbol{M}$, and the toroidal $\boldsymbol{T}$ are shown in the left panel. An atomic force microscope image of the fabricated multiferroic grating and the cross-sectional depth profile along the a-axis are shown in the right panel. Excerpt from [29]. Reprinted with permission from [29]. Copyright 2006 by the American Physical Society.

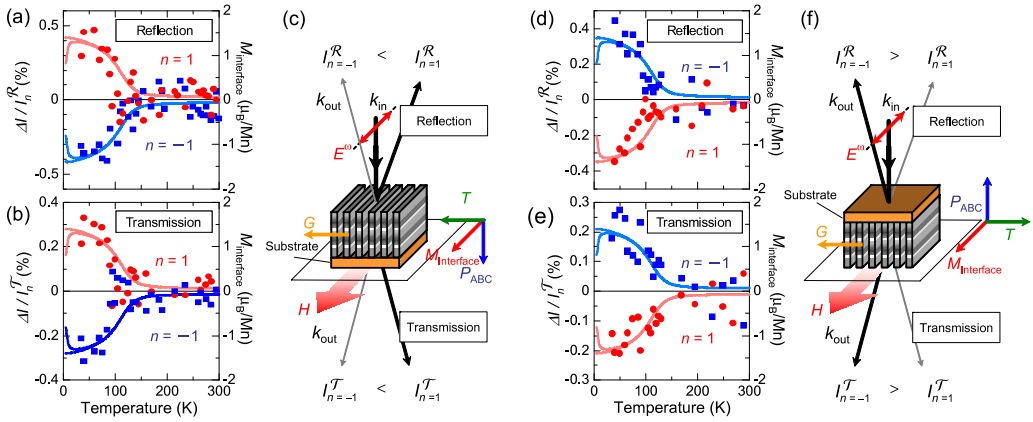

Figure 9. Temperature dependence of relative change in diffracted light intensity $\Delta I_n/I_n$ (circles and squares) in a grating made of asymmetric superlattice (SL) for Bragg spots of the order $n = \pm 1$ with reversal of the magnetic field H (2 kOe) in (a) reflection and (b) transmission geometries. The SL consists of 10 repeated sequences of six-unit-cell $LaMnO_3$, four-unit-cell $SrMnO_3$, and two-unit-cell $LaAlO_3$, which can break the space-inversion symmetry, represented symbolically by the effective polarization $\boldsymbol{P}_{\rm ABC}$. The period of the fabricated grating is 4 μm. The temperature dependence of the magnetization of the SL is also shown for comparison as solid lines. (c) Schematics of Bragg diffraction from the grating in transmission and reflection geometries. Toroidal $\boldsymbol{T}$ is parallel or anti-parallel to the reciprocal lattice vector $\boldsymbol{G}$ of the grating. The polarization $\boldsymbol{E}^{\omega}$ of the incident laser is fixed to the direction of $\boldsymbol{H}$. Results obtained when the sample was turned upside down are also shown in (d)–(f). Excerpt from [31]. Reprinted with permission from [31]. Copyright 2007 by the American Physical Society.

$\boldsymbol{P}_{\rm ABC}$ can be embedded in such a SL. If the SL includes ferromagnetic material as a component, it can behave as a multiferroic. This artificial multiferroicity was first reported by Ogawa *et al*, who observed the magnetic second-harmonic generation of light and related non-linear magneto-optical Kerr effect (NOMOKE) in a $SrTiO_3/LaAlO_3/La_{0.6}Sr_{0.4}MnO_3$ SL on a $SrTiO_3$ substrate [30]. Observation of linear ME optics in such an artificial multiferroic is, however, not simple, when the magnetization vector $\boldsymbol{M}$ is perpendicular to $\boldsymbol{P}_{\rm ABC}$, because the light with a propagation vector parallel to $\boldsymbol{P}_{\rm ABC}$ cannot be modulated. One can overcome this problem by fabricating a grating. As in the case of the grating on the (010) surface of $GaFeO_3$, ME diffraction can be observed even if the incident light is perpendicular to the effective toroidal defined as $\boldsymbol{T}_{\rm eff} \propto \boldsymbol{P}_{\rm ABC} \times \boldsymbol{M}$. Kida *et al* studied ME diffraction from a tailor-made ME grating fabricated in a $LaMnO_3/SrMnO_3/LaAlO_3$ SL [31]. Although none of the three components are ferromagnetic in bulk nature, an interface between antiferromagnetic $LaMnO_3$ and $SrMnO_3$ possesses ferromagnetic moments below 150 K [32]. Such interface magnetism may be strongly coupled with the potential gradient and result in a fairly large toroidal moment. Figure 9 shows that the intensities of diffracted beams in both reflection and transmission modes are modulated by an order of 10^{-3} with the reversal of interface magnetization. The sign of the change in intensity is completely determined by the relative relation

between the propagation vector of the diffracted beam and $\boldsymbol{T}$, as predicted, corroborating the theory that the magnetic modulation is caused by the ME susceptibility of the diffracted beam in the artificial SL.

5. Conclusion

To date, there have been only a limited number of reports published on ME optics, partly because the effect was believed to be quite small. However, a breakthrough has recently been made in non-centrosymmetric ferromagnetic materials. In particular, the observance of large non-reciprocal directional dichroism in CuB_2O_4 might stimulate interest in multiferroics in both scientific and technological fields. A lack of suitable ME materials has also prevented an extensive study from being carried out in this field. The latest progress in nano-technology can assist in the fabrication of tailor-made ME materials, which makes it possible to produce ME diffraction and magnetic second-harmonic generation as linear and non-linear ME optics, respectively. The absorption and diffraction of x-rays related to the linear ME effect can be used as a unique probe into the arrangement of toroidal moments, not only in multiferroics but also in antiferro-toroidic materials.

Acknowledgments

The author would like to thank Y Tokura, M Kubota, J H Jung, N Kida, T Yamada, H Sato, H Akoh, H Yamada, M Kawasaki, J P He, X Z Yu, Y Kaneko, M Matsubara, Y Shimada, S Murakami, N Nagaosa, M. Saito, and K. Taniguchi. Measurements of non-reciprocal x-ray directional dichroism and magnetic x-ray diffraction were performed at the Photon Factory, KEK, Japan. The presented studies were partly supported by the ERATO 'spin-superstructure' project of Japan Science and Technology, and Grants-in-Aid from the Ministry of Education, Culture, Sports, Science and Technology, Japan.

References

[1] Brown W F Jr, Shtrikman S and Treves D 1963 *J. Appl. Phys.* **34** 1233
[2] Pisarev R V, Krichevtsov B B and Pavlov V V 1991 *Phase Transit.* **37** 63
[3] Krichevtsov B B, Pavlov V V, Pisarev R V and Gridnev V N 1993 *J. Phys.: Condens. Matter* **5** 8233
[4] Astrov D N 1960 *Zh. Exp. Teor. Fiz.* **38** 984
Astrov D N 1960 *Sov. Phys.—JETP* **11** 708 (Engl. Transl.)
[5] Rivera J-P 1994 *Ferroelectrics* **161** 165
[6] Schmid H 2001 *Ferroelectrics* **252** 253
[7] Spaldin N A, Fiebig M and Mostovoy M 2008 *J. Phys.: Condens. Matter* **20** 434203
[8] Rikken G L J A and Raupach E 1998 *Phys. Rev.* E **58** 5081
[9] Remeika J P 1960 *J. Appl. Phys.* **31** S263
[10] Rado G T 1964 *Phys. Rev. Lett.* **13** 335
[11] Kubota M, Arima T, Kaneko Y, He J P, Yu X Z and Tokura Y 2004 *Phys. Rev. Lett.* **92** 137401
[12] Arima T, Higashiyama D, Kaneko Y, He J P, Goto T, Miyasaka S, Kimura T, Oikawa K, Kamiyama T, Kumai R and Tokura Y 2004 *Phys. Rev.* B **70** 064426
[13] Popov Yu F, Kadomtseva A M, Vorob'ev G P, Timofeeva V A, Ustinin D M, Zvezdin A K and Tegeranchi M M 1998 *Zh. Éksp. Teor. Fiz.* **114** 263
Popov Yu F, Kadomtseva A M, Vorob'ev G P, Timofeeva V A, Ustinin D M, Zvezdin A K and Tegeranchi M M 1998 *J. Exp. Theor. Phys.* **87** 146 (Engl. Transl.)
[14] Van Aken B B, Rivera J P, Schmid H and Fiebig M 2007 *Nature* **449** 702
[15] Di Matteo S, Joly Y and Natoli C R 2005 *Phys. Rev.* B **72** 144406
[16] Di Matteo S and Joly Y 2006 *Phys. Rev.* B **74** 014403
[17] Jung J H, Matsubara M, Arima T, He J P, Kaneko Y and Tokura Y 2004 *Phys. Rev. Lett.* **93** 037403
[18] Boehm M, Roessli B, Schefer J, Ouladdiaf B, Amato A, Baines C, Staub U and Petrakovskii G A 2007 *Physica* B **318** 277
[19] Kousaka Y, Yano S, Kishine J, Yoshida Y, Inoue K, Kikuchi K and Akimitsu J 2007 *J. Phys. Soc. Japan* **76** 123709
[20] Saito M, Taniguchi K and Arima T 2008 *J. Phys. Soc. Japan* **77** 013705
[21] Rikken G L J A and Raupach E 1997 *Nature* **390** 493
[22] Shimada Y, Matsubara M, Kaneko Y, He J P and Tokura Y 2006 *Appl. Phys. Lett.* **89** 101112
[23] Shimada Y, Kiyama H and Tokura Y 2007 *Phys. Rev.* B **75** 245125
[24] Arima T, Jung J H, Matsubara M, Kubota M, He J P, Kaneko Y and Tokura Y 2005 *J. Phys. Soc. Japan* **74** 1419
[25] Matsubara M, Shimada Y, Arima T, Taguchi Y and Tokura Y 2005 *Phys. Rev.* B **72** 220404R
[26] Kawata H and Mori K 1995 *Rev. Sci. Instrum.* **66** 1407
[27] Kida N, Yamada T, Konoto M, Okimoto Y, Arima T, Koike K, Akoh H and Tokura Y 2005 *Phys. Rev. Lett.* **94** 077205
[28] Sawada K and Nagaosa N 2005 *Appl. Phys. Lett.* **87** 042503
[29] Kida N, Kaneko Y, He J P, Matsubara M, Sato H, Arima T, Akoh H and Tokura Y 2006 *Phys. Rev. Lett.* **96** 167202
[30] Ogawa Y, Yamada H, Ogasawara T, Arima T, Okamoto H, Kawasaki M and Tokura Y 2003 *Phys. Rev. Lett.* **90** 217403
[31] Kida N, Yamada H, Sato H, Arima T, Kawasaki M, Akoh H and Tokura Y 2007 *Phys. Rev. Lett.* **99** 197404
[32] Yamada H, Kawasaki M, Lottermoser T, Arima T and Tokura Y 2006 *Appl. Phys. Lett.* **89** 052506